Enzyme entrapped nanoporous scaffolds formed through flow-induced gelation in a microfluidic filter device for sensitive biosensing of organophosphorus compounds†

Donglai Lu,[a] Guocheng Shao,[b] Dan Du,[ac] Jun Wang,[a] Limin Wang,[a] Wanjun Wang[b] and Yuehe Lin*[a]

Received 25th August 2010, Accepted 10th November 2010
DOI: 10.1039/c0lc00337a

A novel and versatile processing method was developed for the formation of gel scaffolds with *in situ* AChE–AuNPs immobilization for biosensing of organophosphorus compounds. The biosensor designed by our new approach shows high sensitivity, selectivity and reactivation efficiency. This flow-induced immobilization technique opens up new pathways for designing a simple, fast, biocompatible, and cost-effective process for enhanced sensor performance and on-site monitoring of a variety of toxic organophosphorus compounds.

There has been an increasing priority in environmental monitoring to develop a fast and reliable sensor assay to identify and assess site contamination of organophosphorus (OP) compounds.[1–3] In biosensor detection, enzyme-based biosensors have emerged the past few years as the most promising alternative for direct monitoring of pesticides. Various inhibition biosensor systems, based on the immobilization of acetylcholinesterase (AChE) onto various electrochemical or optical transducers, have been proposed for field screening of OP neurotoxins.[4–10] In spite of significant advances made recently in this area, the design of a highly efficient and cost-effective technique that can be reliably deployed in immobilization of AChE or other biomolecules still faces formidable challenges.[11,12] These challenges include complicated and costly fabrication procedures, non-uniform distribution of immobilized AChE in the host matrix along with the enzyme's low stabilities and bioreactivities. Furthermore, the host matrices are often not highly biocompatible and bristle in nature.

Nanomaterial based biosensors are evolving as promising alternatives for rapid, inexpensive, sensitive and accurate identification of individual exposure to OPs. Recent advances in nanotechnology have stemmed the creation of diverse nanostructures by utilizing unique features of microfluidic devices with superior control of reactions, both kinetic and thermodynamic.[13] These characteristics of the nanomaterials have offered enormous prospects in designing novel methods of enzyme immobilization in biosensor devices. Here, we present a novel and versatile flow-induced gelation method to immobilize AChE–gold nanoparticle conjugates (AChE–AuNPs) inside nanogel scaffolds in microfluidic filter device.

[a]*Pacific Northwest National Laboratory, Richland, WA, 99352, USA. E-mail: yuehe.lin@pnl.gov*
[b]*Department of Mechanical Engineering, Louisiana State University, Baton Rouge, LA, USA*
[c]*Key Laboratory of Pesticide and Chemical Biology of Ministry of Education, College of Chemistry, Central China Normal University, Wuhan, 430079, P.R. China*

† Electronic supplementary information (ESI) available: Supplementary procedures, Figures and video. See DOI: 10.1039/c0lc00337a

The novel enzyme immobilization method introduced here is based on recent work of forming stable gel scaffolds with proper hydrodynamic conditions for a given self assembly precursor in microporous flow.[14] When subject to flow, flow-induced structure (FIS) formation of self assembled surfactant micelles occurs in a narrow range of concentrations of specific ionic surfactant solutions with added salts. Existing work on phase transitions in macroscopic geometry, has been reported to be reversible under shear flow conditions.[15] However, the major challenge of utilizing shear induced structures as gel scaffolds is the structure breakdown and the disintegration once the flow is stopped. We are able to obtain irreversible gel scaffolds by using a specially designed microfluidic filter (see Fig. 1). The irreversible gel formation results from the large shear and extension strain rates and total strain generated by the flow through the microstructure, under mixed extensional and shear flow conditions. Based on the previous report for our precursor (surfactant–salt mixture),[14–17] it was identified that the irreversible gelation conditions were, with a critical shear rate of $\sim$10 s^{-1}, a critical strain of $\sim$5000, and a critical extension rate of $\sim 10^6$ s^{-1}.

In the previous report, numerous smaller channels have been made by inserting polydispersed (20–100 μm) glass particles (Polysciences, PA) inside the microchannel to achieve the large strain values required for FIS formation (see ref. 14). A small amount of these particles was added before injecting the precursor solution. The channels were designed with a constriction to hold the particles. Under flow, these particles accumulated near the constriction and formed a nonhomogeneous packed bed. However, as the packing is not ideal, a few large gaps between the channel and the particles allow

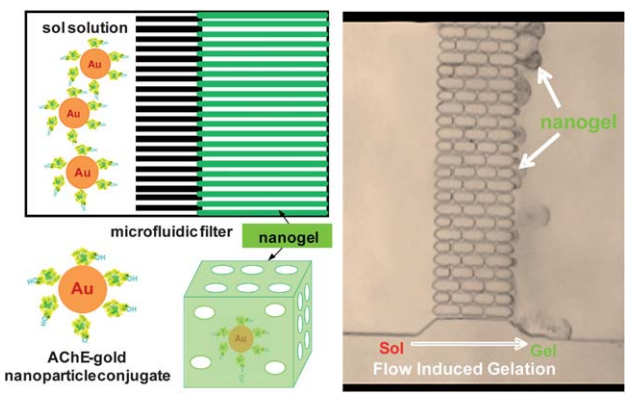

Fig. 1 Schematic diagram of flow-induced gelation in a microfluidic filter device (left) and typical microscope image showing the nanogel production at a flow rate of 10 ml h^{-1} (right). The sol solution contains CTAB at a concentration of $C_1 = 0.003$ M, CMC $\sim$ 0.0009 M, NaSal at $C_2 = 0.003$ M, AChE–AuNPs at $C_3 = 1$ mg ml^{-1}.

some of the incoming fluid to pass through without being sufficiently strained. As a result, the gelation efficiency is very low with this setup. Also, the procedure to prepare a pseudo-packed bed in a microchannel is complicated, and the formed microporous structure is usually uncontrollable. Moreover, the glass particles may attach or be entrapped inside the nanogel which makes the separation step more challenging. To meet these challenges, we employed a modern microfabrication technique to achieve the critical shear rates and strain for irreversible gelation in a microfluidic filter device for FIS formation. As the precursor passes through these narrow channels, the shear rates and extension rates shoot up by several orders of magnitude exceeding the strains required for irreversible gel formation. Compared with the previous pseudo-packed bed, the microfluidic filter device can achieve a higher gelation efficiency, the process for nanogel production is much faster, easier and controllable. In short, we are able to use a microfluidic filter device to create a purely flow-induced, high extension-dominated flow (extension rate $\gg 1 \times 10^6\ s^{-1}$), allowing the surfactant solution to undergo permanent gelation and form stable, biocompatible gel scaffolds under ambient conditions. In this work, we tested microfluidic filter devices with different gap sizes including 3, 10 and 15 μm, and only observed the irreversible gel formation results from the device with 3 μm gaps.

Fig. 1A shows the schematic representation of the microfluidics filter device for continuous production of gel material. The nanostructures of the gel have been exploited in the previous publication.[14] In summary, the gel consists of highly aligned micelles with a short-range order. The alignment of the micelles results in the formation of nano-channels and hole-like regions. Image analysis yields the average nano-channel spacing being 41 ± 6 nm while the pore sizes are 27 ± 4 nm. The nanoporous scaffold formation enabled by microfluidics offers an ideal encapsulating environment for enzymes and many other biomolecules.

In this work, we adopted the microfluidic filter system for flow-induced gelation approach to encapsulate AChE–AuNPs inside gel scaffolds in a single step. The gold colloid (8.5–12.0 nm mean particle size) was purchased from Sigma-Aldrich. The synthesis of AChE–AuNPs conjugates was described in details elsewhere.[18] We mixed the AChE–AuNPs with the surfactant and salt as the precursor solution (or sol) before they pass through the microfluidics setup (see Fig. 1). The gel obtained after the sol passes through microchannels provides a host matrix with AChE–AuNPs immobilized inside the porous scaffolds. This novel flow-induced gelation technique relied purely on fluid mechanics, which allows entrapped enzymes to retain their functional characteristics to a large extent.

The conventional sol–gel procedures generally rely on either acid or base as a catalyst and use alcoholic solvents that usually result in entrapped biomolecules being partially denatured and aggregated,[19–22] while for our new approach, the flow-induced gel scaffolds synthesis is facilitated and controlled by fluid mechanics with minimal or no usage of chemical and thermal means, and completely biocompatible.

To verify the formation of AChE–AuNPs conjugates and the encapsulation of AChE–AuNPs inside the gel scaffolds, Fig. 2 shows the absorbance spectra of the AChE–AuNPs conjugate (b). Absorption peaks of AChE at 280 nm and gold at 530 nm clearly indicate the formation of AChE–AuNPs conjugates. It also shows the results after the flow-induced gelation procedure with AChE–AuNPs encapsulated (d). Absorption peak of AChE at 280 nm has been overlapped by NaSal, but the gold at 530 nm can be used to verify the effective encapsulation of AChE–AuNPs into the gel matrix by the microfluidics setup.

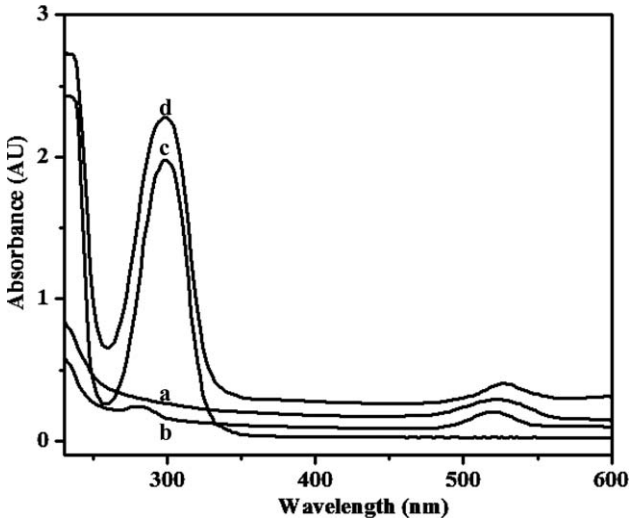

Fig. 2 Absorbance of gold nanoparticles (a), AChE–AuNPs conjugates (b), flow-induced gel material without (c) and with (d) AChE–AuNPs encapsulated. Experimental conditions are the same as those in Fig. 1.

Here, the flow-induced gelation approach enables the entrapment of the AChE–AuNPs into gel scaffolds and offers the following advantages. First, our encapsulation technique is independent of the functionalities on the enzyme. Second, physical entrapment rendered in our approach is functionally noninvasive and preserves the integrity and directional homogeneity of the AChE surface microstructure. In contrast, covalent attachment of AChE *via* surface modification fixes the orientation of the exposed AChE and in certain cases may block substrate access to the AChE's active site.[23,24] In addition, the existing method of physical adsorption of an enzyme inside a nanotube or other porous material[25] is limited by the size of the pores and of the enzyme to be trapped, while our flow-enhanced gelation method is largely independent of the size of the enzyme because the matrix forms around the AChE–AuNPs during the gelation process. Moreover, the flow-induced gel scaffolds can effectively prevent the self aggregation of AChE–AuNPs, but allow the small molecules such as OPs to permeate by simple diffusion.[14,22] In addition, the gel scaffolds can contain a sufficient amount of trapped interstitial water to form a more stable aqueous microenvironment to maintain the AChE's bioactivity.

After we obtain the gel with immobilized AChE–AuNPs, we coat it onto a screen-printed electrode (SPE) for electrochemical detection of OPs model compound of paraoxon. 1 μL gel was cast onto the working electrode surface, and formed a thin layer to cover the top of the electrode. Cyclic voltammetric measurements were firstly used to understand the effects of OP exposure on AChE activity, as shown in Fig. 3. When the gel sensor was exposed to 1 nM paraoxon for 15 min before adding 5 mM ATCh, the peak current greatly decreased (c) compared to the response in the absence of paraoxon (b). Paraoxon as a model OP clearly reduced the enzymatic activity of AChE. This indicates that the gel coated biosensor can be utilized for the detection of trace levels of OPs. However, after addition of 5 mM 2-PAM to the inhibited AChE solution for 15 min, the peak current regained nearly completely to control levels (green line), indicating that the inhibited AChE had been completely reactivated by 2-PAM.

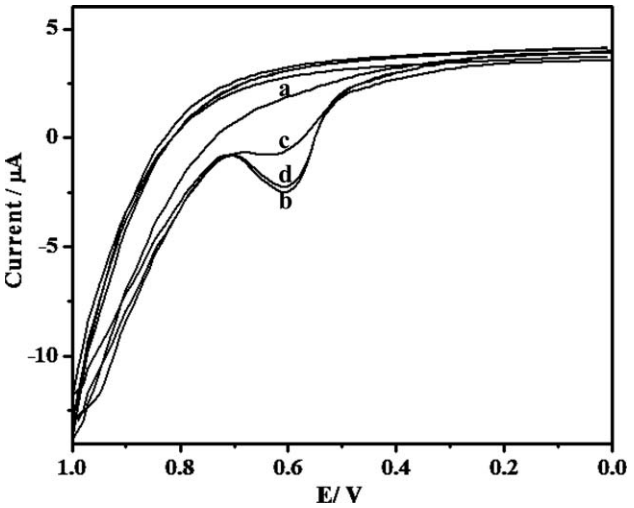

Fig. 3 Cyclic voltammograms of 5 mM ATCh at gel modified electrodes in PBS (a), and gel with AChE–AuNPs encapsulated in PBS without paraoxon exposure (b), in PBS with 1 nM paraoxon exposure for 15 min (c) and following reactivation by 5 mM 2-PAM incubation for 15 min (d). Experimental conditions are the same as those in Fig. 1.

We also compared the amperometric response of our gel based paraoxon sensor and sensor fabricated by chitosan for sensitivity study using a dual-working electrode in a flow injection analysis system.[5] For comparison purposes, we used the same initial AChE–AuNPs concentration in the chitosan solution and the precursor solution for the gel production. The chitosan based sensor is a widely used method for enzyme immobilization by entrapment.[26] For both sensors, successive injections of 5 mM ATCh after exposure to different levels of paraoxon were performed, as shown in Fig. 4. For the chitosan based paraoxon sensor (A), an insignificant current response and poor reactivation were observed after the addition of 25 pM paraoxon and 5 mM 2-PAM. In contrast, a larger and well-defined current response (close to 4 times higher) was obtained with the gel modified SPE (B) with the same AChE–AuNPs content inside the gel matrix. Moreover, the AChE's activity can be almost totally restored with the reactivation procedure for the nanogel sensor. The performance displayed in Fig. 4 shows that the gel based sensor exhibits higher sensitivity and reactivation efficiency compared to the chitosan based sensor. The possible reason could be that the gel with an immobilized enzyme can usually provide a more stable aqueous microenvironment, which is of utmost importance for maintaining the native stabilities and reactivities of AChE. As in an aqueous medium, the side chains of AChE interact with solvent water through hydrogen bonding and dipolar interactions. The OP recognition sites of the AChE are almost always exposed on the surface, and its sensitivity is usually maximized in an aqueous medium, which also allows the 2-PAM molecules to easily access the inhibited AChE to reactivate the AChE's activity.[22,27] The simple, gold nanoparticle mediated, immobilization method fabricates highly homogeneous AChE–AuNPs arrays with higher capacities than those prepared by using conventional techniques, and can give an enhancement to sensor performance.[18]

The calibration plot of the paraoxon biosensor was shown in Fig. 4C. As expected, the response of the gel based biosensor (a) to

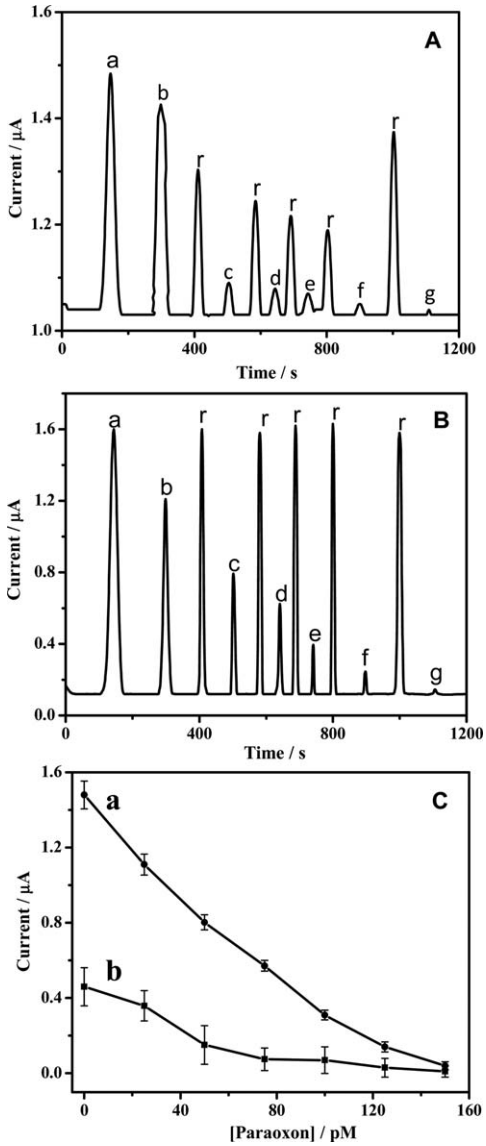

Fig. 4 Amperometric responses of 5 mM ATCh at chitosan (A) and gel (B) modified SPE (operated at +0.6 V) in PBS with exposure to 0, 25–150 pM (a, b–g) paraoxon for 15 min, along with the reactivation of AChE by 5 mM 2-PAM incubation for 15 min (r). The calibration curve of the biosensor is shown in C. Other conditions, as in Fig. 1.

paraoxon was linear in the experimental range of 25–200 pM with a detection limit of 6 pM (10% signal drop), while the chitosan based sensor (b) only has a detection limit of 30 pM.

The gel based enzymatic biosensor enables direct measurements of OPs in relevant environmental samples. For example, Fig. 5 demonstrates the suitability of the new gel based protocol for measuring paraoxon in natural waters. This Figure shows results for an untreated river water sample (a), and following spiking it with increasing concentrations of paraoxon in 20 pM steps (b–f). The sample contained moderately high fully dissolved solids (~1500 mg L^{-1}). The successful test of paraoxon with our gel based biosensor demonstrates its promise for sensitive monitoring of OPs in a field environment.

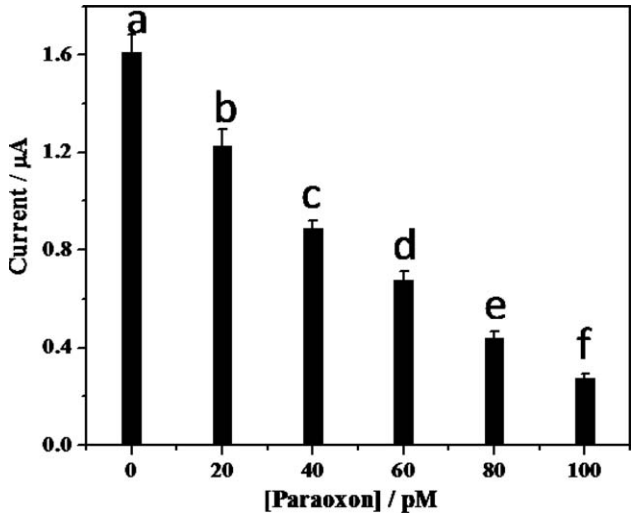

Fig. 5 The amperometric signals of 5 mM ATCh with increasing 20 pM paraoxon spiked in untreated river water sample (b–f) along with the background current (a). The river water was 10-fold diluted, then different amounts of paraoxon were spiked into this diluted river water to final concentrations of 20–100 pM. The reactivation data was not shown. Other conditions, as in Fig. 4.

Conclusions

In conclusion, we present a flow-induced gelation method with the immobilization of AChE–AuNPs inside a gel matrix and its application in monitoring organophosphorus compounds. Our new approach takes advantage of unique microfluidic filter structures to facilitate the single throughput, *in situ* process to immobilize AChE–AuNPs in a gel scaffold. The flow-induced gel scaffold's synthesis purely relied on fluid mechanics, with no usage of chemical and thermal means, is completely biocompatible, and can retain the AChE's native stabilities and bioactivities. The high sensitivity and reactivation efficiency of this biosensor stems from the unique properties of the gel scaffold that provides essentially the same local aqueous microenvironment as in biological media, while providing the favourable host matrix that isolates the AChE–AuNPs, protecting them from self aggregation and leaching. This flow-induced immobilization technique of utilizing a microfluidic filter device thus opens up new pathways for designing a simple, fast, biocompatible, and cost-effective process for enhanced sensor performance and on-site monitoring of a variety of OPs.

Acknowledgements

This work was done at Pacific Northwest National Laboratory (PNNL) and was supported partially by PNNL's Laboratory Directed Research and Development Program and by Grant Number U01 NS058161-01 from the NIH's CounterAct Program through the National Institute of Neurological Disorders and Strokes, NIH. PNNL is operated for the U.S. Department of Energy (DOE) by Battelle under Contract DE-AC05-76RL01830. The characterization was performed using EMSL, a national scientific user facility sponsored by the Department of Energy's Office of Biological and Environmental Research and located at PNNL. Dan Du would like to acknowledge the financial support by the Program for Chenguang Young Scientist for Wuhan (200950431184) and the National Natural Science Foundation of China (21075047).

Notes and references

1 A. T. J. Dale and A. Rebek, *Angew. Chem.*, 2009, **48**, 7850.
2 J. Wang, G. Liu, C. Timchalk and Y. Lin, *Environ. Sci. Technol.*, 2008, **42**, 2688.
3 C. Timchalk, A. Busby, J. A. Campbell, L. L. Needham and D. B. Barr, *Toxicology*, 2007, **237**, 145.
4 S. A. Melnychuk, A. A. Neverov and R. S. Brown, *Angew. Chem.*, 2006, **45**, 1767.
5 D. Du, J. Wang, J. N. Smith, C. Timchalk and Y. H. Lin, *Anal. Chem.*, 2009, **81**, 9314.
6 F. Worek, U. Mast, D. Kiderlen, C. Diepold and P. Eyer, *Clin. Chim. Acta*, 1999, **288**, 73.
7 G. D. Liu and Y. H. Lin, *Anal. Chem.*, 2006, **78**, 835.
8 F. Worek, G. Reiter, P. Eyer and L. Szinicz, *Arch. Toxicol.*, 2002, **76**, 523.
9 J. F. Payne, A. Mathieu, W. Melvin and L. L. Fancey, *Mar. Pollut. Bull.*, 1996, **32**, 225.
10 S. Hudson, J. Cooney and E. Magner, *Angew. Chem.*, 2008, **47**, 8582.
11 U. T. Bornscheuer, *Angew. Chem.*, 2003, **42**, 3336.
12 X. H. N. Xu and E. S. Yeung, *Science*, 1998, **281**, 1650.
13 Y. J. Song, J. Hormes and C. S. S. R. Kumar, *Small*, 2008, **4**, 698.
14 M. Vasudevan, E. Busel, D. L. Lu, A. Q. Shen, B. Khomami and R. Sureshkumar, *Nat. Mater.*, 2010, **9**, 436.
15 C. H. Liu and D. J. Pine, *Phys. Rev. Lett.*, 1996, **77**, 2121.
16 A. Onuki, *J. Phys.: Condens. Matter*, 1997, **9**, 6119.
17 M. Vasudeven, A. Q. Shen, B. Khomami and R. Sureshkumar, *J. Rheol.*, 2008, **52**, 527.
18 X. Mao, Y. Q. Ma, A. G. Zhang, L. R. Zhang, L. W. Zeng and G. D. Liu, *Anal. Chem.*, 2009, **81**, 1660.
19 M. T. Reetz, A. Zonta and J. Simpelkamp, *Biotechnol. Bioeng.*, 1996, **49**, 527.
20 G. Z. Cao, Y. F. Lu, L. Delattre, C. J. Brinker and G. P. Lopez, *Adv. Mater.*, 1996, **8**, 588.
21 U. Narang, P. N. Prasad, F. V. Bright, K. Ramanathan, N. D. Kumar, B. D. Malhotra, M. N. Kamalasanan and S. Chandra, *Anal. Chem.*, 1994, **66**, 3139.
22 B. C. Dave, B. Dunn, J. S. Valentine and J. I. Zink, *Anal. Chem.*, 1994, **66**, 1120A.
23 C. Kronman, O. Cohen, L. Raveh, O. Mazor, A. Ordentlich and A. Shafferman, *Toxicology*, 2007, **233**, 40.
24 P. Skladal and M. Mascini, *Biosens. Bioelectron.*, 1992, **7**, 335.
25 P. Xiao, B. B. Garcia, Q. Guo, D. W. Liu and G. Z. Cao, *Electrochem. Commun.*, 2007, **9**, 2441.
26 D. Du, X. Huang, J. Cai, A. D. Zhang, J. W. Ding and S. Z. Chen, *Anal. Bioanal. Chem.*, 2007, **387**, 1059.
27 S. Yang, W. Z. Jia, Q. Y. Qian, Y. G. Zhou and X. H. Xia, *Anal. Chem.*, 2009, **81**, 3478.

